Cell Reports

Article

Glia Promote Synaptogenesis through an IQGAP PES-7 in *C. elegans*

Graphical Abstract

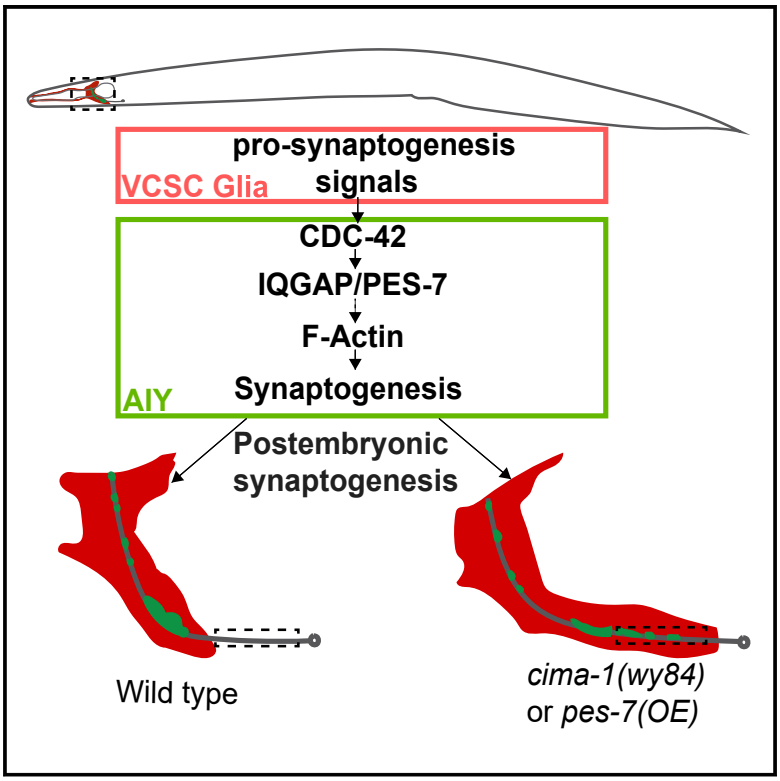

Authors

Xiaohua Dong, Shuhan Jin, Zhiyong Shao

Correspondence

shaozy@fudan.edu.cn

In Brief

Dong et al. reveal a role of the conserved CDC-42 and IQGAP/PES-7 in glia-mediated synaptogenesis during postembryonic development. At the glia-neurite contact sites, PES-7 activated by CDC-42 promotes presynaptic formation, possibly through regulating the F-actin assembly, providing insight into the neuronal responses to pro-synaptic signaling from glia.

Highlights

- CDC-42 and IQGAP PES-7 are required for glia-mediated synaptogenesis
- PES-7 acts downstream of CDC-42 to promote synaptic formation
- CHD and GRD domains of PES-7 are required for synaptogenesis
- PES-7 promotes synaptogenesis, most likely through F-actin

Dong et al., 2020, Cell Reports *30*, 2614–2626
February 25, 2020
https://doi.org/10.1016/j.celrep.2020.01.102

CellPress

OPEN ACCESS
CellPress

Cell Reports
Article

Glia Promote Synaptogenesis through an IQGAP PES-7 in *C. elegans*

Xiaohua Dong,[1] Shuhan Jin,[1] and Zhiyong Shao[1,2,*]
[1]Department of Neurosurgery, State Key Laboratory of Medical Neurobiology and MOE Frontiers Center for Brain Science, Institutes of Brain Science, Zhongshan Hospital, Fudan University, Shanghai 200032, China
[2]Lead Contact
*Correspondence: shaozy@fudan.edu.cn
https://doi.org/10.1016/j.celrep.2020.01.102

SUMMARY

Synapses are fundamental to the normal function of the nervous system. Glia play a pivotal role in regulating synaptic formation. However, how presynaptic neurons assemble synaptic structure in response to the glial signals remains largely unexplored. To address this question, we use *cima-1* mutant *C. elegans* as an *in vivo* model, in which the astrocyte-like VCSC glial processes ectopically reach an asynaptic neurite region and promote presynaptic formation there. Through an RNAi screen, we find that the Rho GTPase CDC-42 and IQGAP PES-7 are required in presynaptic neurons for VCSC glia-induced presynaptic formation. In addition, we find that *cdc-42* and *pes-7* are also required for normal synaptogenesis during postembryonic developmental stages. PES-7 activated by CDC-42 promotes presynaptic formation, most likely through regulating F-actin assembly. Given the evolutionary conservation of CDC-42 and IQGAPs, we speculate that our findings in *C. elegans* apply to vertebrates.

INTRODUCTION

Synapses are specialized structures that allow electrical or chemical signals to pass from neurons to their target cells. They are formed with remarkable specificity at both cellular and subcellular levels (Huang, 2006; White, 2007; Williams et al., 2010; Yogev and Shen, 2014). After their formation, synapses remain dynamic, undergoing processes that include maturation, pruning, and experience-dependent reshaping (Bosworth and Allen, 2017; Neniskyte and Gross, 2017). While prior research has identified molecules regulating synaptic formation and stability (Chai et al., 2017; Lin and Koleske, 2010; Melom and Littleton, 2011; Shi et al., 2012), less is known about the maintenance of synaptic spatial specificity during postnatal growth.

Glia play vital roles in synaptic formation and maintenance (Bosworth and Allen, 2017; Neniskyte and Gross, 2017). Astrocytes express secreted and adhesion molecules, including thrombospondins, glypicans, SPARC1, neuroligins, which promote or suppress synaptic formation, maturation, or elimination (Christopherson et al., 2005; Garrett and Weiner, 2009; Göritz et al., 2002; Kucukdereli et al., 2011; Stogsdill et al., 2017). In addition, astrocytes provide spatial cues for synaptogenesis (Hochstim et al., 2008; Molofsky et al., 2014; Tsai et al., 2012). Glial contributions to synaptic development are evolutionally conserved in invertebrates such as *Drosophila* and *Caenorhabditis elegans* (Colón-Ramos et al., 2007; Muthukumar et al., 2014). Despite the vital role of glia in synaptogenesis, the molecular mechanisms by which neurons assemble synapses in response to glial signaling remain unclear.

We previously identified a sialin homolog, CIMA-1, required for astrocyte-like VCSC (ventral cephalic sheath cell) glia-mediated synaptic position maintenance (Shao et al., 2013). In *cima-1* mutants, VCSC glia promote synaptogenesis by making ectopic contact with the neurites of AIY interneurons during postembryonic development, which provides an excellent model to address the mechanisms underlying glia-mediated synaptogenesis during postembryonic development (Shao et al., 2013). Through an RNAi screen, we found that *cdc-42* and *pes-7*, which encode a Rho guanosine triphosphatase (GTPase) and an IQ GTPase activation protein (IQGAP), respectively, are required in the presynaptic neurons for the glia-mediated synaptic formation.

IQGAPs are evolutionarily conserved scaffold proteins that contain a calponin homology domain (CHD) at the N terminus, IQ and GAP-related domains (GRDs) in the middle, and a Ras GTPase-activating protein-C-terminal domain (RasGAP-C) at the C terminus. Through these domains, IQGAPs bind a variety of partners to modulate diverse cellular functions (Cao et al., 2015; Hedman et al., 2015; Jausoro et al., 2012; Smith et al., 2015). In the nervous system, IQGAPs regulate memory formation and neurite growth (Gao et al., 2011; Jausoro et al., 2013; Schrick et al., 2007; Swiech et al., 2011; Wang et al., 2007). However, their roles in presynaptic development remain largely unknown.

The present study shows that the AIY ectopic synaptogenesis induced by VCSC glia in *cima-1* mutants requires CDC-42 and the only IQGAP PES-7 in *C. elegans*. In addition, we found that both CDC-42 and PES-7 are required for synaptogenesis in different types of neurons during postembryonic stages in wild-type (WT) animals. Mechanistically, PES-7 activated by CDC-42 promotes presynaptic assembly, most likely by regulating F-actin polymerization at the glia-neuron contact sites.

RESULTS

CDC-42 and PES-7 Are Required for *cima-1(wy84)* Ectopic Synaptogenesis

To understand the molecular mechanisms underlying glia-mediated synaptogenesis during postembryonic stages, we used

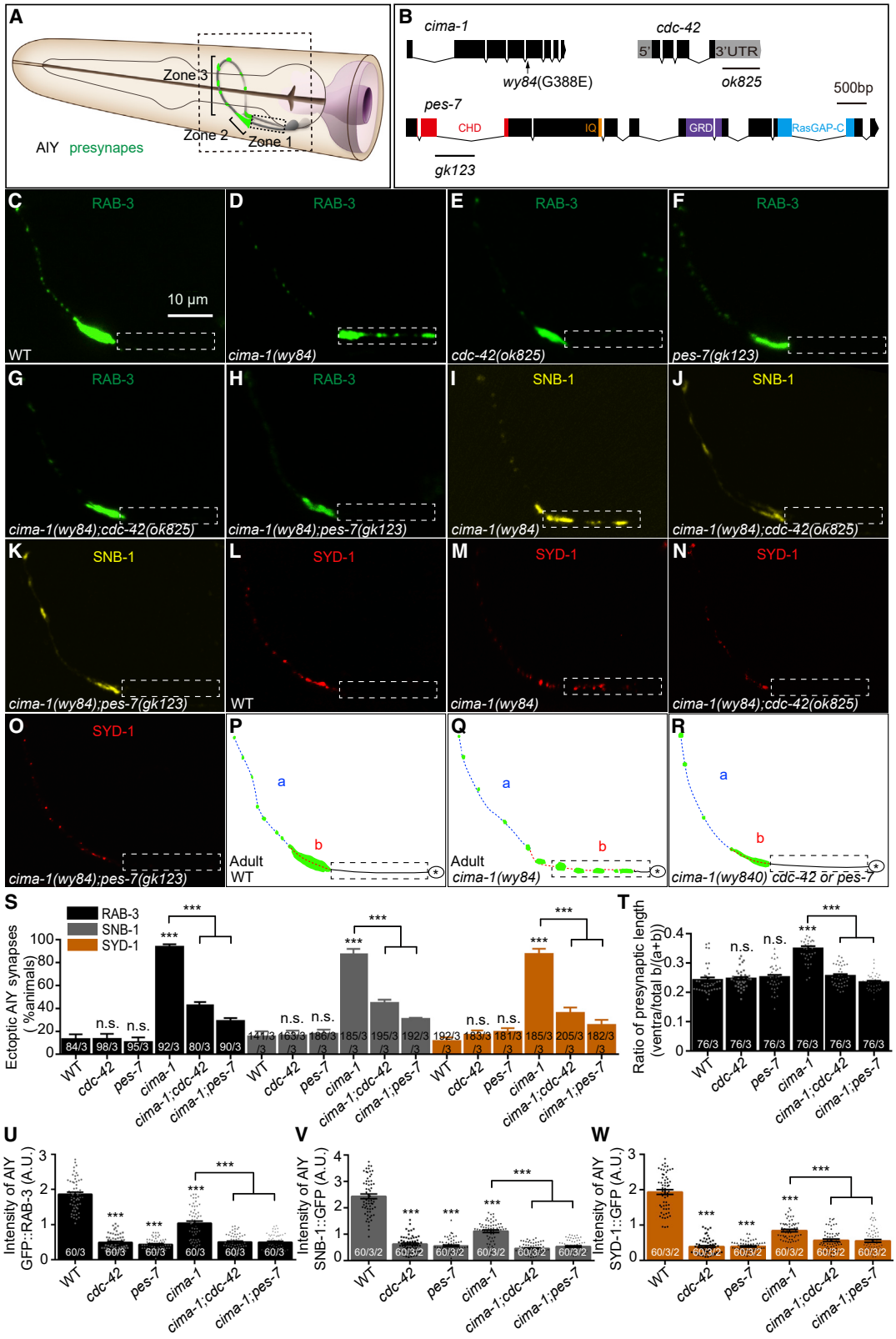

(legend on next page)

C. elegans AIY interneurons as a model. Anatomically, AIY can be divided into three zones: the ventral region proximal to soma called zone 1, the distal region innervated in the nerve ring called zone 3, and the region connecting zones 1 and 3 called zone 2. The presynaptic distribution in AIY is stereotypic. Zone 1 is asynaptic, zone 2 is enriched with synapses, and zone 3 has only a few synaptic sites (Figures 1A and 1C; White et al., 1986; Colón-Ramos, 2009). This presynaptic pattern is already established by larval stage 1 (L1) (Shao et al., 2013; Colón-Ramos et al., 2007). While the AIY neurites and synaptic regions increase as the animals grow from L1 to adult stages, the presynaptic distribution is maintained (Figures S1B–S1B''; Shao et al., 2013).

Previously, we demonstrated that CIMA-1, a member of the SLC17A5 family, regulates AIY presynaptic spatial specificity by maintaining VCSC glial morphology during postnatal development (Shao et al., 2013). While AIY presynaptic distribution is normal at the L1 or the L4 stage, ectopic synapses emerge at the adult stage, partially due to the VCSC glia extension in *cima-1(wy84)* mutants (Figures 1D and S1C–S1C''; Shao et al., 2013). Therefore, the *cima-1(wy84)* mutants provide an excellent model to address the mechanisms by which VCSC glia promote synaptogenesis during postembryonic growth. To identify the genes required for the interaction between glia and neurons, we performed a candidate RNAi suppressor screen in *cima-1(wy84)* mutants (Figures S1A and S1A'). We focused on adhesion molecules and their interaction molecules because the ectopic synapses in *cima-1(wy84)* form at the glia-neuron contact sites (Table S1; Shao et al., 2013). In addition to adhesive molecules, we identified 2 adhesion regulators, CDC-42 and PES-7, which are the evolutionarily conserved Rho GTPase and IQGAP, respectively (Figures S1D–S1H; Table S1). We focused on *cdc-42* and *pes-7* for further studies because they are important signaling molecules and could link the extracellular glia signaling to the presynaptic assembly.

To validate the RNAi data, we analyzed the effect of *cdc-42(ok825)* and *pes-7(gk123)* deletion mutations on the synaptic distribution (Figure 1B). First, we validated the RNAi results in the *cdc-42(ok825)* and *pes-7(gk123)* with the synaptic vesicle GFP::RAB-3 marker, and we found that while both mutations do not affect the distribution of synaptic markers, they robustly suppress the ectopic synapses of *cima-1(wy84)* mutants, which are consistent with the RNAi data (Figures 1C–1H and 1S). Second, we examined additional presynaptic markers, including synaptic vesicle protein SNB-1 and the active zone protein SYD-1. Consistently, both SNB-1 and SYD-1 markers are suppressed by *cdc-42(ok825)* or *pes-7(gk123)* (Figures 1I–1O, 1S, and S2A–S2D''). Finally, we examined the suppression, with postsynaptic RIA neurons as a reference. RIA neurons innervate with AIY in the zone 2 region in WT animals, and the AIY presynapses extend beyond the AIY and RIA contact in *cima-1(wy84)* (Shao et al., 2013). We found that either *cdc-42(ok825)* or *pes-7(gk123)* suppresses the ectopic synapses beyond the contact area (Figures S2E–S2H). Since all of the synaptic markers tested showed consistent results, we only used the integrated GFP::RAB-3 marker for most of the rest of the analysis for convenience.

To further confirm the *cima-1* suppression role of *cdc-42* and *pes-7*, we quantified the expressivity of the suppression effect of *cdc-42(ok825)* and *pes-7(gk123)* on *cima-1(wy84)* by calculating the ratio of the ventral:total synaptic lengths (see Method Details; Shao et al., 2013). While the ratio in the *cdc-42(ok825)* and *pes-7(gk123)* mutants is similar to that in WT animals (0.23, 0.24, and 0.24 in WT, *cdc-42(ok825)*, and *pes-7(gk123)* mutants, respectively) ($p = 0.29$ and 0.17 for *cdc-42(ok825)* and *pes-7(gk123)* as compared to WT, respectively; Figure 1T), we found that both robustly suppress the ratio of *cima-1(wy84)* mutants (0.35, 0.24, and 0.24 in *cima-1(wy84)*, *cima-1(wy84);cdc-42(ok825)* and *cima-1(wy84);pes-7(gk123),* respectively) ($p < 0.001$ for both double mutants compared to *cima-1(wy84)*; Figure 1T).

The above data showed that both *cdc-42(ok825)* and *pes-7(gk123)* suppress the ectopic synapses in *cima-1(wy84)* at adult day 1 stage. To exclude the possibility that *cdc-42(ok825)* and *pes-7(gk123)* delay the ectopic synapse development, we examined the suppression effect until adult day 5 stage and found that the degree of suppression remained until then (Figure S3), which

Figure 1. CDC-42 and PES-7 Are Required for the Formation of Ectopic Synapses in *cima-1(wy84)* Mutants

(A) Illustration showing the AIY interneurons (gray) in the head of the *C. elegans* (Altun et al., 2002–2019). Presynaptic structures are indicated in green. The AIY neurites are divided into three zones as described in the text and by Shao et al. (2013).

(B) Schematics describe the genomic structures of *cima-1*, *cdc-42*, and *pes-7*. Boxes and lines indicate exons and introns. The conserved calponin homology domain (CHD), IQ domain, GTPase-activating protein-related domain (GRD), and the Ras GTPase-activating protein-C-terminal domain (RasGAP-C) are highlighted in red, orange, purple, and blue, respectively. The *cima-1(wy84)*, *pes-7(gk123)*, and *cdc-42(ok825)* mutant sites are indicated. Scale bar, 500 bp.

(C–O) Confocal micrographs of the AIY presynaptic structure labeled with the synaptic vesicle marker GFP::RAB-3 (green, C–H), SNB-1::YFP (yellow, I–K), or the synaptic active zone marker GFP::SYD-1 (red, L–O) corresponding to the region in the square dashed box in (A). Dashed boxes mark zone 1 of AIY interneurons. The scale bar (10 μm) in (C) applies to (D–O). While synaptic signals are not present in the zone 1in WT (C and L), *pes-7(gk123)* or *cdc-42(ok825)* mutant (E and F), they ectopically emerge in the *cima-1(wy84)* mutants (D, I, and M). The ectopic synapses are suppressed by *pes-7(gk123)* or *cdc-42(ok825)* (G, H, J, K, N, and O).

(P–R) Schematic diagrams of the AIY synaptic distribution in wild type (WT) (P), *cima-1(wy84)* (Q), and *cima-1(wy84);cdc-42(ok825)* or *cima-1(wy84);pes-7(gk123)* (R). a, the length of zone 3; b, the sum of the zone 2 and the ectopic synaptic length in zone 1.

(S) Quantification of the percentage of animals with ectopic AIY presynaptic markers for indicated genotypes.

(T) Quantification of the ratio of ventral synaptic length (b in P–R):total synaptic length (sum of a and b in P–R).

(U–W) Quantification of GFP::RAB-3 (U), SNB-1::YFP (V), and GFP::SYD-1 (W) fluorescence intensity in AIY. The total number of adult day 1 animals (N), the replicates (n1) are indicated in each bar for each genotype, as they are for the transgenic lines created and the number of transgenic lines (n2) examined (all using the convention N/n1/n2).

Statistical analyses are based on 1-way ANOVA followed by Dunnett's test. Error bars represent SEMs; n.s., not significant; ***$p < 0.001$ as compared to WT (if on top of bars), unless brackets are used between 2 compared genotypes.

See also Figures S1, S2, S3, S4, and S5.

excludes the possibility that *cdc-42(ok825)* and *pes-7(gk123)* delay ectopic synapse development in *cima-1(wy84)* mutants. These data collectively demonstrate that *cdc-42* and *pes-7* are required for *cima-1(wy84)*-induced ectopic synaptic formation, as demonstrated in the model (Figures 1P–1R).

CDC-42 and PES-7 Are Required for Normal Synaptogenesis during Postembryonic Stages

The above data show that the AIY synaptic distribution is unaffected in either *cdc-42(ok825)* or *pes-7(gk123)* mutants. To address the physiological role of *cdc-42* and *pes-7*, we quantified the synaptic fluorescence intensity of the synaptic markers in AIY interneurons. The synaptic intensity of all of the synaptic markers tested (including RAB-3, SNB-1, and SYD-1) are significantly reduced in both *cdc-42(ok825)* and *pes-7(gk123)* mutants (Figures 1C, 1E, 1F, and 1U–1W), suggesting that both *cdc-42* and *pes-7* are required for AIY normal synaptogenesis. We noticed that the synaptic intensity was reduced in *cima-1(wy84)* mutants, which is probably the side effect of the spatial maintenance defect. The synaptic intensity was further reduced in both double mutants, which is consistent with the above results that both *cdc-42* and *pes-7* are required for *cima-1(wy84)* ectopic synaptogenesis. The data suggest that *cdc-42* and *pes-7* are required not only for the *cima-1(wy84)* ectopic synaptogenesis but also for WT synaptic formation in the AIY interneurons.

To determine when *cdc-42* and *pes-7* are required for synaptogenesis in WT animals, we quantified the intensity of GFP::RAB-3 at different developmental stages. We found that the GFP intensity is not affected at the newly hatched L1 stage, but significantly reduced at the adult day 1 stage (Figures S4A–S4D), indicating that *cdc-42* and *pes-7* are required for AIY presynaptic assembly specifically during postembryonic stages.

To address whether *cdc-42* and *pes-7* are sufficient to promote synaptogenesis in AIY neurons, we expressed extra copies of *cdc-42* and *pes-7* in WT animals. We found that overexpressing either *cdc-42* or *pes-7* results in ectopic synapses only at the adult stage, not during larval stages, suggesting that the overexpression is sufficient to promote the ectopic synapse formation in AIY (Figure S5A). Furthermore, we found that *pes-7* overexpression, but not *cdc-42* overexpression, significantly increases the GFP::RAB-3 intensity since later larval stage (Figure S5B). These data suggest that overexpressing *pes-7* is sufficient to promote synaptogenesis at the correct position during larval stages, but in the wrong area (zone 1) at the adult stage, indicating its critical roles in regulating synaptic temporal and spatial specificity in AIY interneurons. The reason why *cdc-42* overexpression is not sufficient is probably because it acts upstream in the pathway or its expression or function is strictly regulated.

Next, we wanted to determine whether the role of *cdc-42* and *pes-7* in synaptic assembly is general or AIY specific. We examined the synaptic marker in other neurons, including the interneuron AIB and sensory neurons ASE and AWB. Except for the AIB, whose presynaptic intensity is reduced in *cdc-42(ok825)* at the L1 stage, the intensity of those neurons is not affected at the newly hatched L1 stage, but it is significantly reduced at the adult stage (Figures S4E–S4P). These results suggest that the requirement of *cdc-42* and *pes-7* for presynaptic assembly during postembryonic development is most likely general rather than AIY specific.

cdc-42 and *pes-7* Promote Synaptogenesis in Response to VCSC Glial Signaling

The formation of ectopic synapses in *cima-1(wy84)* mutants is mainly mediated by the contact between the VCSC glia and AIY interneurons (Shao et al., 2013). The suppression of AIY ectopic synapses by *cdc-42(ok825)* or *pes-7(gk123)* could occur either through altering VCSC glial morphology or blocking synaptogenic signaling from the glia. To differentiate these two models, we simultaneously visualized the AIY synaptic marker GFP::RAB-3 and the mCherry-labeled VCSC glia. The glial endfeet only reach zone 2, where synapses are enriched in WT animals (Figures 2A and 2B), which is consistent with previous reports (Shao et al., 2013; White et al., 1986). However, the endfeet extend posteriorly and contact the AIY zone 1 in *cima-1(wy84)* mutants (Figures 2C, 2D, and 2I; Shao et al., 2013). Although both *pes-7(gk123)* and *cdc-42 (ok825)* suppress the ectopic synapses, neither of them suppresses the extension of the glial endfeet of *cima-1(wy84)* mutants (Figures 2E–2J and S6). These data are consistent with the model that *cdc-42* and *pes-7* block synaptogenic signaling downstream of VCSC glia. To further test the model, we ablated VCSC glia by expressing cell apoptosis factors described by Chelur and Chalfie (2007) in *cima-1(wy84)*, *cima-1(wy84);cdc-42(ok825)*, and *cima-1(wy84);pes-7(gk123)* mutants. Our quantitative data show that the degrees of ectopic synapse suppression by the combination of genetic mutations and glia ablation are similar to these just by *pes-7(gk123)* or *cdc-42(ok825)* mutation (Figure 2J). These results collectively suggest that *cdc-42* and *pes-7* act downstream of VCSC glia to promote synaptogenesis in *cima-1(wy84)* mutants.

cdc-42 and *pes-7* Act Cell Autonomously in AIY to Promote Synaptic Formation in *cima-1(wy84)*

To understand where *cdc-42* and *pes-7* act, we sought to determine where *cdc-42* and *pes-7* are expressed. We found that P*cdc-42::GFP* is broadly expressed in early embryogenesis (Figures S7A–S7E). In larval and adult stages, the reporter is highly enriched in the nervous system (Figures S7E–S7E'; data not shown), which is consistent with previous reports (Neukomm et al., 2014). Similarly, P*pes-7::pes-7::GFP* expression begins at the gastrulation stage in only a few cells (Figure S7F) and broadens as the embryo develops (Figures S7G–S7I). Consistent with its roles in cell adhesion, PES-7::GFP localizes to the cell cortex (Figures S7G–S7I). In the larval or adult stages, the expression of P*pes-7::pes-7::GFP* is also enriched in the nervous system, with some in the epidermis, muscles, and intestines (Figures S7J–S7J'). Both *cdc-42* and *pes-7* reporters are expressed in the AIY interneurons (Figures S7K–S7P').

Next, we expressed *cdc-42* or *pes-7* cDNA with tissue-specific promoters in the corresponding double mutants. We found that driving either of them expression with its own promoter, the pan-neuronal promoter (P*rab-3*), or the AIY specific promoters (P*ttx-3* or P*mod-1*) rescues and restores the ectopic synapses and the intensity of synaptic markers (Figures 3A–3P), while driving *cdc-42* or *pes-7* under body-wall muscle-, intestine-, or epidermis-specific promoters (P*myo-3,* P*ges-1,* P*dpy-7*

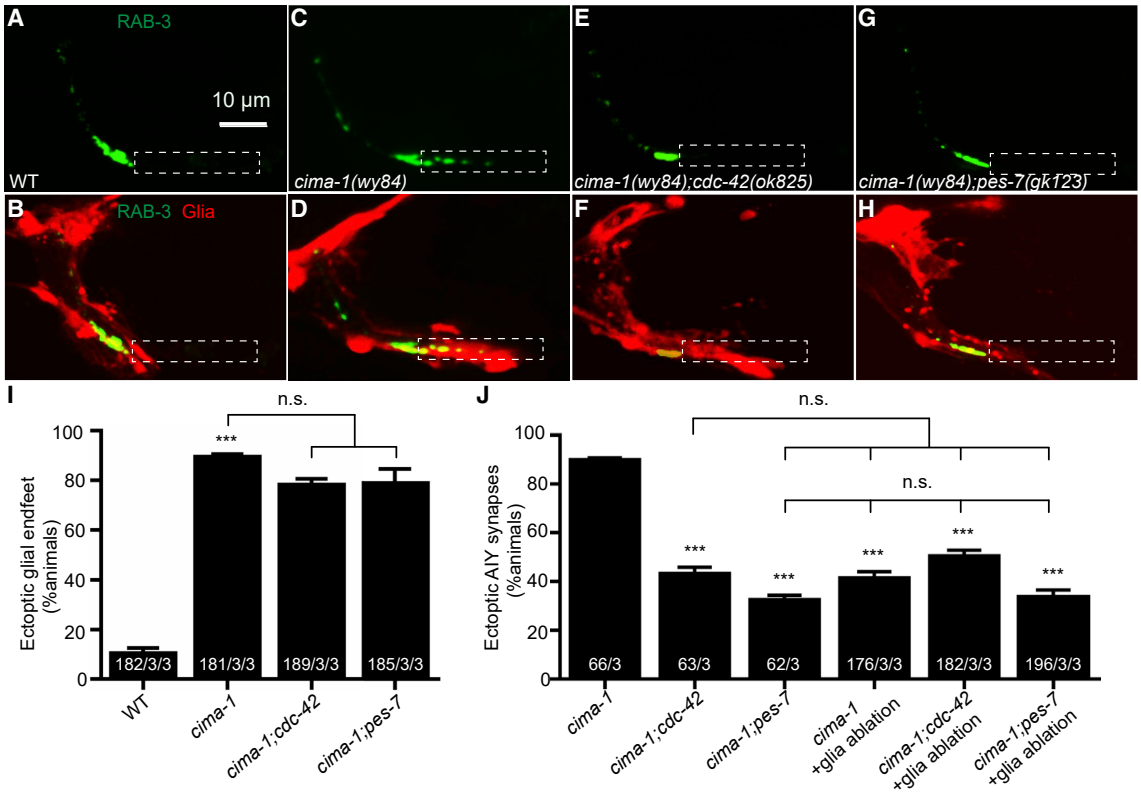

Figure 2. PES-7 and CDC-42 Are Required for VCSC Glia-Mediated Synaptogenesis

(A–H) Confocal micrographs of the AIY presynaptic GFP::RAB-3 marker (A, C, E, and G) and the GFP::RAB-3 with VCSC glia (red in B, D, F, and H) in WT animals (A and B) and *cima-1(wy84)* (C and D), *cima-1(wy84);cdc-42(ok825)* (E and F), and *cima-1(wy84);pes-7(gk123)* mutants (G and H). The scale bar in (A) is 10 μm and applies to (B–H). Dashed boxes mark the area of zone 1 in the AIY interneurons.

(I) Quantification of the percentage of animals with VCSC glial extension into zone 1 for the indicated genotypes.

(J) Quantification of the percentage of animals with ectopic synapses in AIY zone 1 for the indicated genotypes. The total number of adult day 1 animals (N) and the replicates (n1) are indicated in each bar for each genotype, as they are for the transgenic lines created and the number of transgenic lines (n2) examined (all using the convention N/n1/n2).

Statistical analysis is based on 1-way ANOVA followed by Dunnett's test. Error bars represent SEMs; n.s., not significant; ***$p < 0.001$ as compared to WT (I) or *cima-1(wy84)* (J) (if on top of bars), unless brackets are used between 2 compared genotypes.

See also Figure S6.

respectively) does not (Figures 3M–3P). These data indicate that both *cdc-42* and *pes-7* act cell autonomously in the AIY interneurons to promote synaptic formation in *cima-1(wy84)* mutants, which is consistent with the aforementioned model; *cdc-42* and *pes-7* act downstream of VCSC glia.

CDC-42 and PES-7 Localize to Presynaptic Sites

To further understand how CDC-42 and PES-7 promote the ectopic synapse formation, we determined their subcellular localization in AIY interneurons by fusing CDC-42 and PES-7 with mCherry. We expressed the mCherry-fused proteins in the AIY interneurons and found that both CDC-42 and PES-7 are enriched at presynaptic sites, colocalizing with the presynaptic marker GFP::RAB-3 (Figures 4A–4B''). Consistent with the previous overexpression data, mCherry::PES-7 expression in AIY interneurons induces far more ectopic synapses than does the expression of mCherry::CDC-42 (Figures 4A and 4B), suggesting that the mCherry tag does not affect the function of either CDC-42 or PES-7, and the subcellular localizations are most likely to be correct. In addition, when mCherry::PES-7 and GFP::CDC-42 are simultaneously expressed in AIY interneurons, they colocalize (Figures 4C–4C''). These data indicate that both PES-7 and CDC-42 localize to presynaptic sites in the AIY interneurons, promoting synaptic assembly.

PES-7 Acts Downstream of CDC-42 to Promote Synaptic Formation

To determine whether *cdc-42* and *pes-7* act in the same genetic pathway, we generated *cima-1(wy84);cdc-42(ok825);pes-7(gk123)* triple mutants. We found that the degree of ectopic synapse suppression by the double mutations of *pes-7 (gk123)* and *cdc-42 (ok825)* is similar to that achieved by either of the single mutations (Figures 5A–5F), suggesting that *cdc-42* and *pes-7* act in the same genetic pathway to promote synaptic assembly.

IQGAP can be a regulator or an effector of CDC42 (Brown and Sacks, 2006). To determine whether PES-7 acts upstream or downstream of CDC-42, we overexpressed *pes-7* or *cdc-42* in the WT animals, the *cima-1(wy84)* mutants,

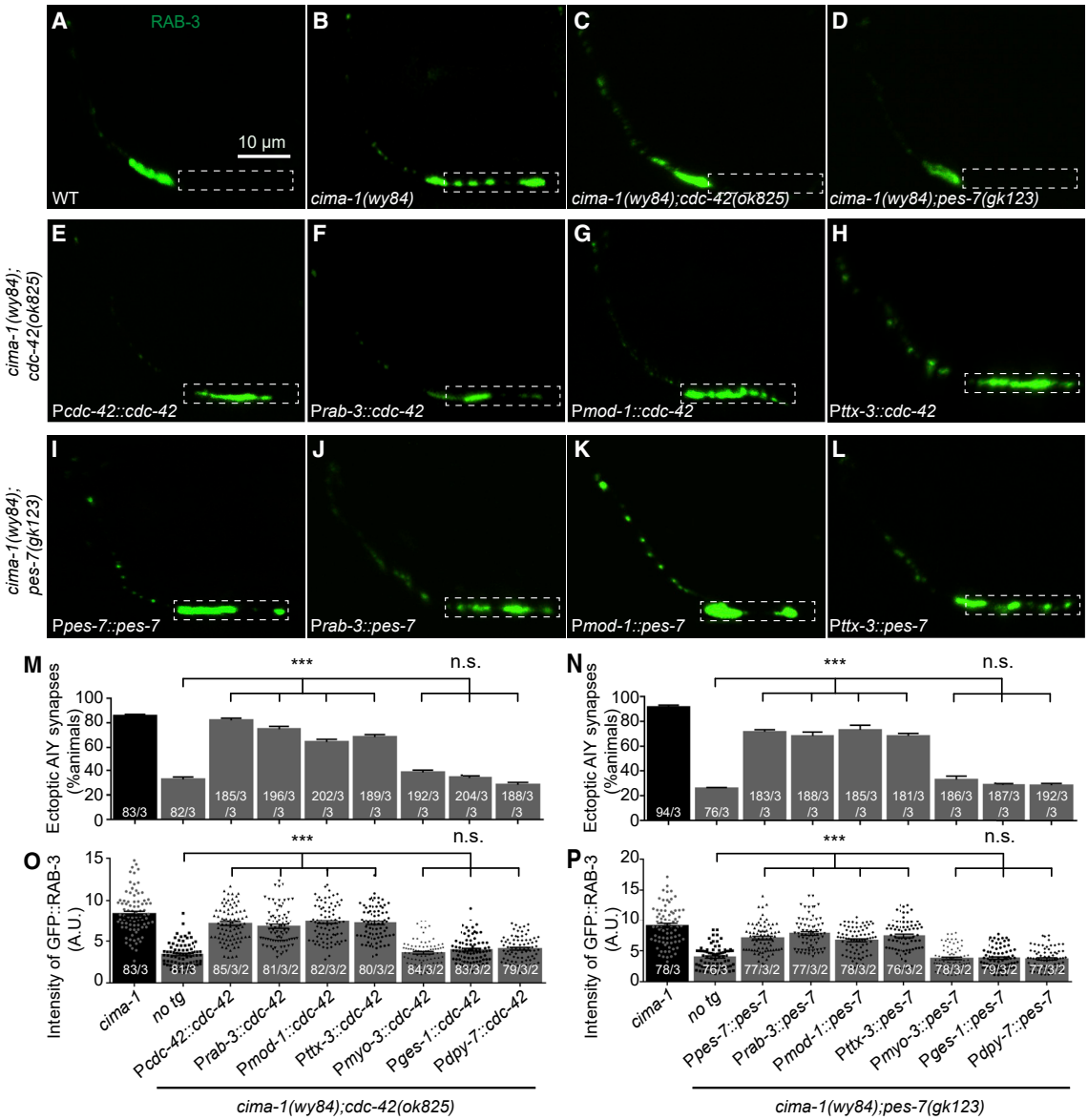

Figure 3. *cdc-42* and *pes-7* Act Cell Autonomously in AIY to Promote *cima-1(wy84)* Ectopic Synaptogenesis

(A–L) Confocal micrographs of AIY labeled with the synaptic vesicle marker GFP::RAB-3 in WT (A) and *cima-1(wy84)* (B), *cima-1(wy84);cdc-42(ok825)* (C), *cima-1(wy84);pes-7(gk123)* (D), *cima-1(wy84);cdc-42(ok825)* mutants with the P*cdc-42::cdc-42* transgene (E), or the tissue-specific *cdc-42* transgenes P*rab-3::cdc-42* (pan-neuronal promoter) (F), P*mod-1::cdc-42* (AIY-specific promoter) (G), and P*ttx-3::cdc-42* (AIY-specific promoter) (H), and *cima-1(wy84);pes-7(gk123)* double mutants with the P*pes-7::pes-7* transgene (I) or the tissue-specific *pes-7* transgenes P*rab-3::pes-7* (pan-neuronal promoter) (J), P*mod-1::pes-7* (AIY specific promoter) (K), and P*ttx-3::pes-7* (AIY specific promoter) (L). Dashed boxes indicate zone 1 of AIY interneurons. The scale bar (10 μm) in (A) applies to (B)–(L).

(M and N) Quantification of the percentage of animals with ectopic AIY presynaptic markers for the indicated genotypes for tissue specific rescue of *cdc-42(ok825)* (M) and *pes-7(gk123)* (N).

(O and P) Quantification of GFP::RAB-3 intensity for tissue-specific rescue of *cdc-42(ok825)* (O) and *pes-7(gk123)* (P) for the indicated genotypes. no tg, no transgene. Tissue-specific promoters include P*rab-3*(neuronal), P*mod-1*(AIY), P*ttx-3*(AIY), P*myo-3*(body wall muscle), P*ges-1*(intestine), and P*dpy-7*(epidermis). The total number of adult day 1 animals (N) and the replicates (n1) are indicated in each bar for each genotype, as they are for the transgenic lines created and the number of transgenic lines (n2) examined (all using the convention N/n1/n2).

Statistical analysis is based on 1-way ANOVA followed by Dunnett's test. Error bars represent SEMs; n.s., not significant; ***$p < 0.001$.

See also Figure S7.

the *cima-1(wy84);cdc-42(ok825)* double mutants, the *cima-1(wy84);pes-7(gk123)* double mutants, and the *pes-7(gk123); cdc-42(ok825);cima-1(wy84)* triple mutants. We found that *pes-7* overexpression results in the robust increase in ectopic synapses at adult stages, but not larval stages, regardless of genetic background—except for *cima-1(wy84)* mutation, which exhibits

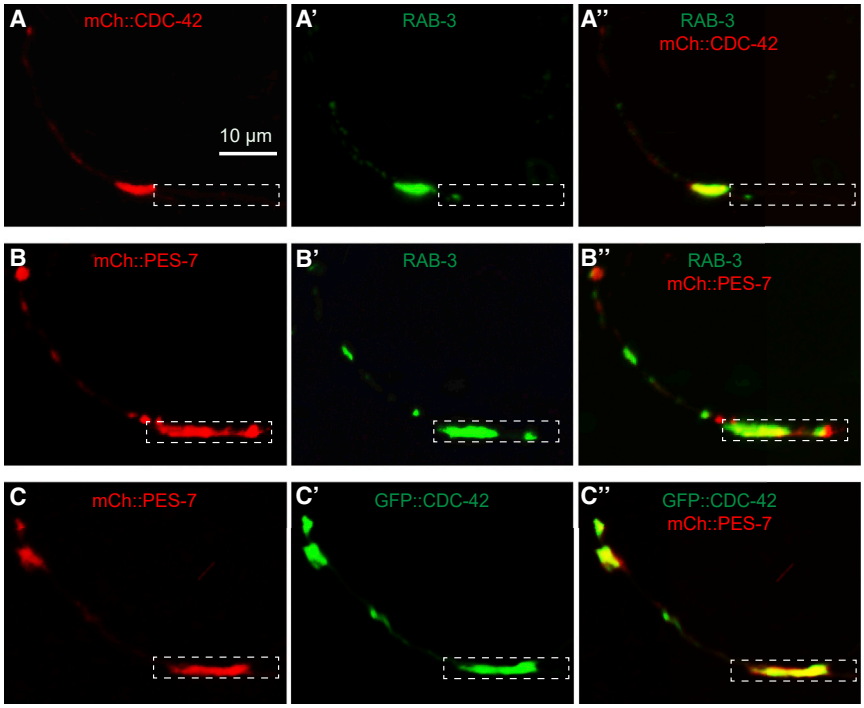

Figure 4. PES-7 and CDC-42 Are Colocalized to the Presynaptic Sites

(A–B'') Confocal micrographs of AIY labeled with mCherry::CDC-42 (A) or mCherry::PES-7 (B) and synaptic vesicle marker GFP::RAB-3 (A' and B') in WT animals. (A'') and (B'') are the merged micrographs.

(C–C'') Confocal micrographs of mCherry::PES-7 (C) and GFP::CDC-42 (C') expression in AIY interneurons. (C'') is the merged channel from (C) and (C'). Dashed boxes indicate zone 1 of the AIY interneurons.

The scale bar (10 μm) in (A) applies to the rest of the panels.

See also Figure S7.

high-penetrance ectopic synapses by itself (Figures 5G). While *cdc-42* overexpression induces only a moderate increase in ectopic synapses in the WT animals and restores the ectopic synaptic distribution in the *cima-1(wy84);cdc-42(ok825)* double mutants, it does not promote the formation of ectopic synapses in *pes-7(gk123)* mutants (Figure 5G). The data indicate that *pes-7* overexpression promotes the ectopic synaptogenesis in a *cdc-42*-independent manner, while *cdc-42* overexpression does so only when *pes-7* is present, suggesting that *pes-7* is required for *cdc-42* function and most likely acts downstream of *cdc-42*.

The Active Form of CDC-42 Is Required to Promote Synaptic Formation

Rho GTPases cycle between the active GTP-bound and the inactive GDP-bound forms (Narumiya, 1996). Single amino acid substitution of these GTPases could result in either constitutively active (Q61L or G12V) or inactive (T17N) forms (Ahmadian et al., 1997; Muraoka et al., 2012). To address whether the CDC-42 active form is required for promoting synaptic formation in *cima-1(wy84)* mutants, we expressed either CDC-42 (Q61L) or CDC-42 (T17N) in the *cima-1(wy84);cdc-42(ok825)* double mutants (Figure 6A). We found that the active form of CDC-42 (Q61L) rescues *cdc-42(ok825)* and restores the ectopic synaptic structures in the double mutants, while the inactive form of CDC-42 (T17N) does not (Figure 6B). In addition, we observed that CDC-42 (T17N) acts as a dominant-negative mutant and suppresses the ectopic synapses in *cima-1(wy84)*, which phenocopies the *cdc-42(ok825)* loss-of-function mutants (Figure 6B). These data suggest that the active form of CDC-42 is required for ectopic synapse formation in *cima-1(wy84)* mutants.

The CHD and GRD Domains of PES-7 Are Required for Promoting Synaptic Formation

Similar to IQGAPs in mammals, PES-7 contains CHD, IQ, GRD, and RasGAP-C domains (Weissbach et al., 1994; Mateer et al., 2004; Figure 6C). To determine which domain of PES-7 is required to promote ectopic synaptic formation in *cima-1(wy84)* mutants, we generated the PES-7 truncation constructs ΔCHD, ΔIQ, ΔGRD, and ΔRasGAP-C and a fragment containing only the CHD and upstream sequences (Figure 6C). We tested the function of these deletion variations of PES-7 in WT or *cima-1(wy84);pes-7(gk123)* double mutants. The function of PES-7 is not affected when IQ or RasGAP-C is deleted. However, the function is completely abolished when CHD, GRD, or both are deleted (Figures 6D and 6E). These results indicate that both CHD and GRD are required for the ectopic synaptic formation in *cima-1(wy84)* mutants.

PES-7 Promotes Presynaptic Formation, Most Likely by Regulating F-Actin Assembly

IQGAPs interact with a variety of partners through different domains (Hedman et al., 2015; Smith et al., 2015). The data above demonstrate that the pro-synaptogenesis function of PES-7 requires the CHD domain, which can interact with and promote F-actin assembly (Jausoro et al., 2013). To determine whether F-actin assembly is associated with presynaptic formation in AIY interneurons, we visualized F-actin with GFP-tagged utrophin (Burkel et al., 2007). We found that, akin to the synaptic distribution, the utrophin localizes to the AIY interneuron synaptic zones 2 and 3, but not to the asynaptic zone 1 in WT animals and *pes-7(gk123)* or *cdc-42(ok825)* single mutants (Figures 7A, 7B, and 7G). Similarly, the ectopic utrophin emerges at zone 1 in *cima-1(wy84)* adults, but is significantly suppressed by *cdc-42(ok825)*, *pes-7(gk123)*, or *pes-7(gk123);cdc-42(ok825)* double mutations (Figures 7C–7E). These data support the hypothesis that CDC-42 and PES-7 promote presynaptic formation by regulating F-actin assembly. To test this model further, we quantified the intensity of utrophin::GFP. Consistent with the

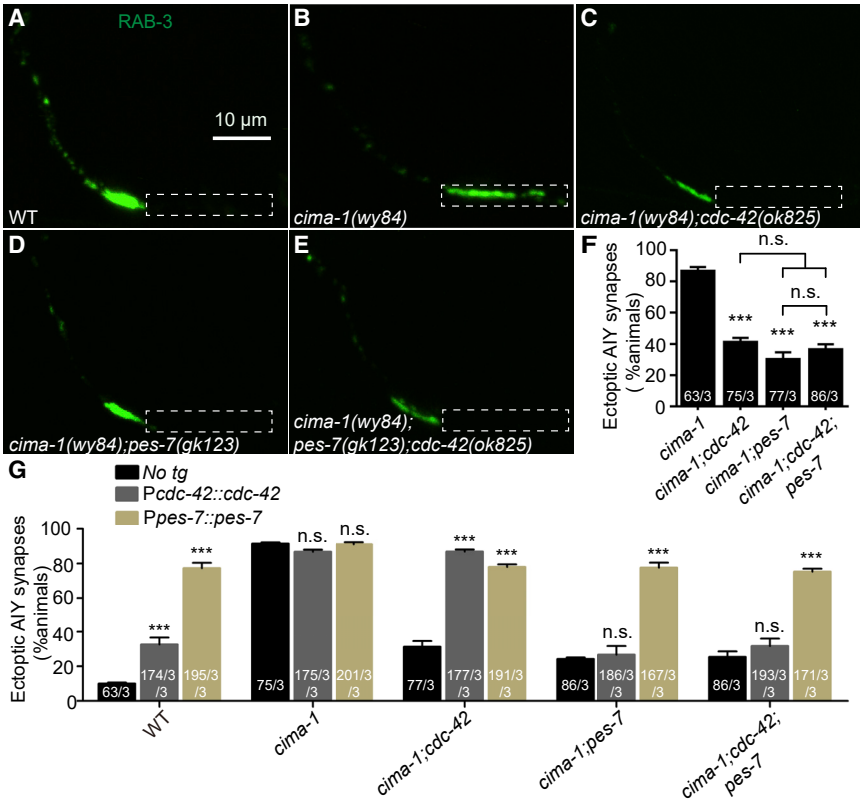

Figure 5. *pes-7* Functions Downstream of *cdc-42* to Promote Synaptic Formation

(A–E) Confocal micrographs of AIY interneurons labeled with synaptic vesicle marker GFP::RAB-3 in WT animals (A), *cima-1(wy84)* single mutants (B), *cima-1(wy84);cdc-42(ok825)* double mutants (C), *cima-1(wy84);pes-7(gk123)* double mutants (D), and *cima-1(wy84);cdc-42(ok825);pes-7(gk123)* triple mutants (E). Dashed boxes mark zone 1 of the AIY interneurons. The scale bar (10 μm) in (A) applies to (B–E).

(F) Quantification of the percentage of animals with ectopic synapses for (B)–(E).

(G) Quantification of the percentage of animals with ectopic AIY GFP::RAB-3 for the indicated genotypes. The statistical analysis was based on 1-way ANOVA (F) or 2-way ANOVA (G), followed by Dunnett's test; Error bars represent SEMs; n.s., not significant; ***$p < 0.001$ as compared to *cima-1(wy84)* (F) or no tg (G) (if on top of bars), unless brackets are used between 2 compared genotypes.

The total number of animals (N) and the replicates (n1) are indicated in each bar for each genotype, as they are for the transgenic lines created and the number of transgenic lines (n2) examined (all using the convention N/n1/n2).

See also Figures S2 and S5.

intensity of synaptic markers, both *cdc-42(ok825)* and *pes-7(gk123)* significantly reduce the F-actin in either WT or *cima-1(wy84)* mutant background (Figure 7H), suggesting that both *cdc-42* and *pes-7* are required for F-actin assembly. In addition, we found that overexpressing *pes-7* is sufficient to promote F-actin assembly as assayed by the utrophin::GFP localization and intensity (Figures 7F–7H). These results consistently support a model in which *cdc-42* and *pes-7* promote synaptic formation by assembling F-actin.

Our results so far support a model in which, in response to VCSC glial signaling, CDC-42 and PES-7 promote synaptic formation at the correct zone 2 position in WT animals during postembryonic development stages and at the ectopic zone 1 position in *cima-1(wy84)* mutants, most likely through assembling F-actin (Figure 7I).

DISCUSSION

Glia play critical roles in synaptogenesis in both vertebrates and invertebrates (Bosworth and Allen, 2017; Colón-Ramos, 2009; Muthukumar et al., 2014). In *C. elegans*, the astrocyte-like VCSC glia secrete netrin to guide axonal growth and promote synaptogenesis during embryogenesis (Colón-Ramos et al., 2007). Local netrin modulates the receptor UNC-40 clustering, which then regulates synaptic formation during the embryonic stage through CED-10/RAC1 and MIG-10/Lamellipodin (Stavoe et al., 2012). During postnatal growth, VCSC glia-neuron contact is required for maintaining synaptic position (Shao et al., 2013). The present study demonstrates that VCSC glia-neuron contact activates IQGAP PES-7 through the GTPase CDC-42 at presynaptic sites, which then promotes synaptogenesis, most likely through regulating F-actin assembly.

In HSN motor neurons, the presynaptic formation through the WVE-1/WAVE complex-mediated local assembly of F-actin (Chia et al., 2014). The local F-actin then recruits active zone proteins SYD-1 and SYD-2 through the neurabin NAB-1 adaptor (Chia et al., 2012). AIY interneuron presynaptic assembly in the embryonic stage is also achieved through F-actin (Stavoe and Colón-Ramos, 2012). Therefore, the role of F-actin in presynaptic assembly could be a general mechanism used in different neuron types and cross-developmental stages.

VCSC Glia Promote Synaptogenesis through CDC-42 and IQGAP/PES-7

In this study, we demonstrated that CDC-42 and PES-7 are required for VCSC glia-mediated synaptogenesis. Three lines of evidence support this. First, the knocking down or loss-of-function mutation of *cdc-42* or *pes-7* suppresses the *cima-1(wy84)* mutation-induced ectopic synapse formation, but not the glial extension; second, expressing *cdc-42* or *pes-7* in AIY interneurons restores the ectopic synapses in the corresponding double mutants; and third, CDC42 and PES-7 are localized to presynaptic sites in AIY neurons.

C. elegans CDC-42, first described in 1993 (Chen et al., 1993), regulates many cellular behaviors, including cell polarity, invasion, and neuronal protrusion (Gotta et al., 2001; Dyer et al., 2010; Kay and Hunter, 2001; Qiu et al., 2000; Lohmer et al., 2016; Alan et al., 2013). In mammals, the homolog CDC42 also regulates

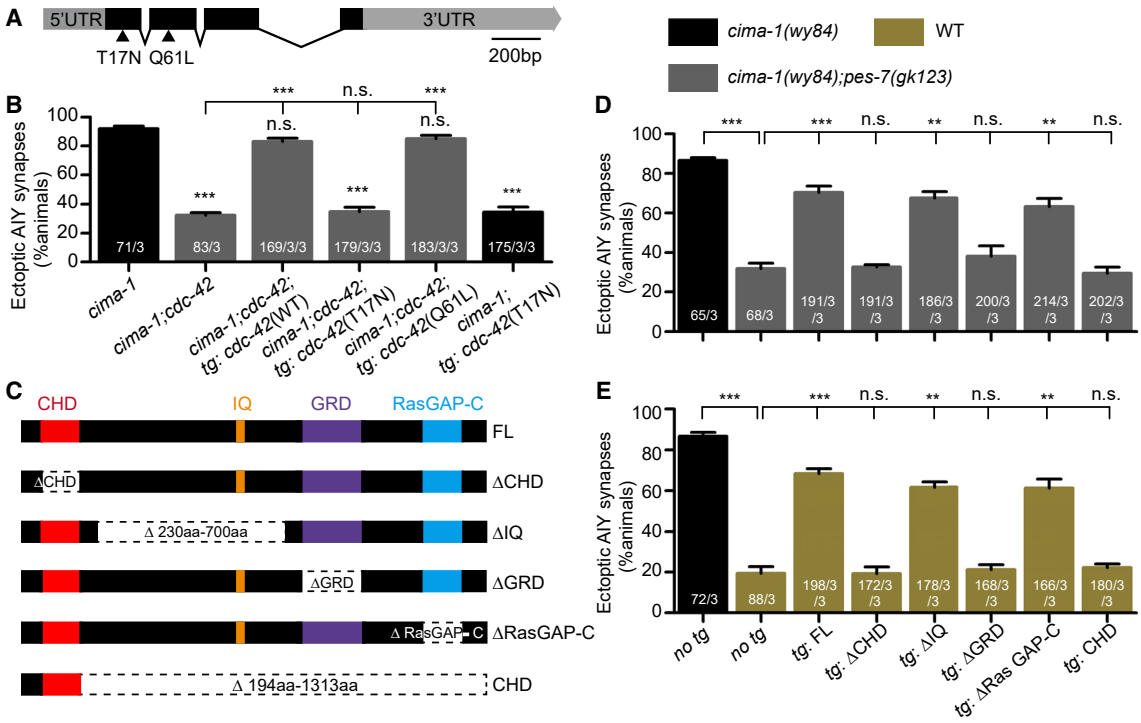

Figure 6. The Active Form of CDC-42 and the CHD and GRD Domains of PES-7 Are Required for Ectopic-Synaptic Formation

(A) A schematic description of the *cdc-42* genomic structure and locations of the constitutive-active (Q61L) and dominant-inactive (T17N) sites.

(B) Quantification of the percentage of animals with ectopic AIY presynaptic markers for the indicated genotypes.

(C) A schematic of full-length and truncated PES-7 mutant forms, including the full-length (FL), CHD deletion (ΔCHD, deletion of the 29th–194th amino acid), IQ domain deletion (ΔIQ, deletion of amino acids 230–700), GRD domain deletion (ΔGRD, deletion of amino acids 765–1,096), RasGAP-C domain deletion (-ΔRasGAP-C, deletion of amino acids 1,178–1,313), and the CHD fragment with only the CHD and the upstream sequences (CHD, deletion of amino acids 194–1,390).

(D and E) Quantification of the percentage of animals with ectopic AIY presynapses for the indicated genotypes. tg, transgene; no tg, no transgene. The total number of animals (N) and the replicates (n1) are indicated in each bar for each genotype, as they are for the transgenic lines created and the number of transgenic lines (n2) examined (all using the convention N/n1/n2).

Statistical analysis is based on 1-way ANOVA followed by Dunnett's test. Error bars represent SEMs; n.s., not significant; $^{**}p < 0.01$, $^{***}p < 0.001$.

dendritic spine formation and plasticity (Tashiro et al., 2000; Tolias et al., 2011; Hedrick et al., 2016; Martin-Vilchez et al., 2017; Murakoshi et al., 2011; Bijata et al., 2017). Recently, CDC42 was also found to be required for presynaptic development in *Drosophila* and mice (Imai et al., 2016; Rodal et al., 2008), indicating that its roles in presynaptic assembly are evolutionarily conserved.

CDC-42 promotes presynaptic assembly through PES-7, an IQGAP that regulates cytoskeleton dynamics under both normal and pathological conditions (Hedman et al., 2015; Watanabe et al., 2015; Lee et al., 2012). In the vertebrate nervous system, IQGAPs regulate dendritic spine formation and morphogenesis (Gao et al., 2011; Jausoro et al., 2013). In *C. elegans*, we found that PES-7 regulates presynaptic assembly in response to glia signaling. Along with the finding that PES-7 regulates cell cytokinesis and possibly GABAergic synaptic vesicle trafficking (Locke et al., 2009; Skop et al., 2004), these data indicate that the role of PES-7 in synaptogenesis is highly conserved.

Spatiotemporal Regulation of Synaptic Assembly

Synaptic connections are precisely regulated at both temporal and spatial levels. The AIY presynaptic distribution of *C. elegans* is established during embryogenesis and maintained thereafter (Shao et al., 2013). During embryogenesis, AIY synaptic formation is mainly regulated by Netrin/UNC-6 signaling (Colón-Ramos et al., 2007). In this study, we found that both CDC-42 and PES-7 are required for postembryonic synaptic formation. In addition, when PES-7 is overexpressed or overactivated, ectopic synapses form, and the AIY synaptic spatial specificity is compromised specifically at the adult stage. These results suggest that CDC-42 and PES-7 play a critical role in the synaptic spatiotemporal specificity. We also showed that the role of PES-7 in synaptogenesis is not AIY specific, but more general.

In vertebrates, astrocytes play critical roles in synaptic formation and plasticity (Alan et al., 2018; Baldwin and Eroglu, 2017). Recent studies revealed that astrocytes are spatially diverse, providing spatial cues for synaptogenesis (Molofsky et al., 2014). However, how presynaptic neurons respond to astrocytic cues to assemble synaptic structure remains unknown. VCSC glia in *C. elegans* are similar to astrocytes in vertebrates from the aspects of origins, function, and transcription profiling (Colón-Ramos et al., 2007; Katz et al., 2018; Katz et al., 2019).

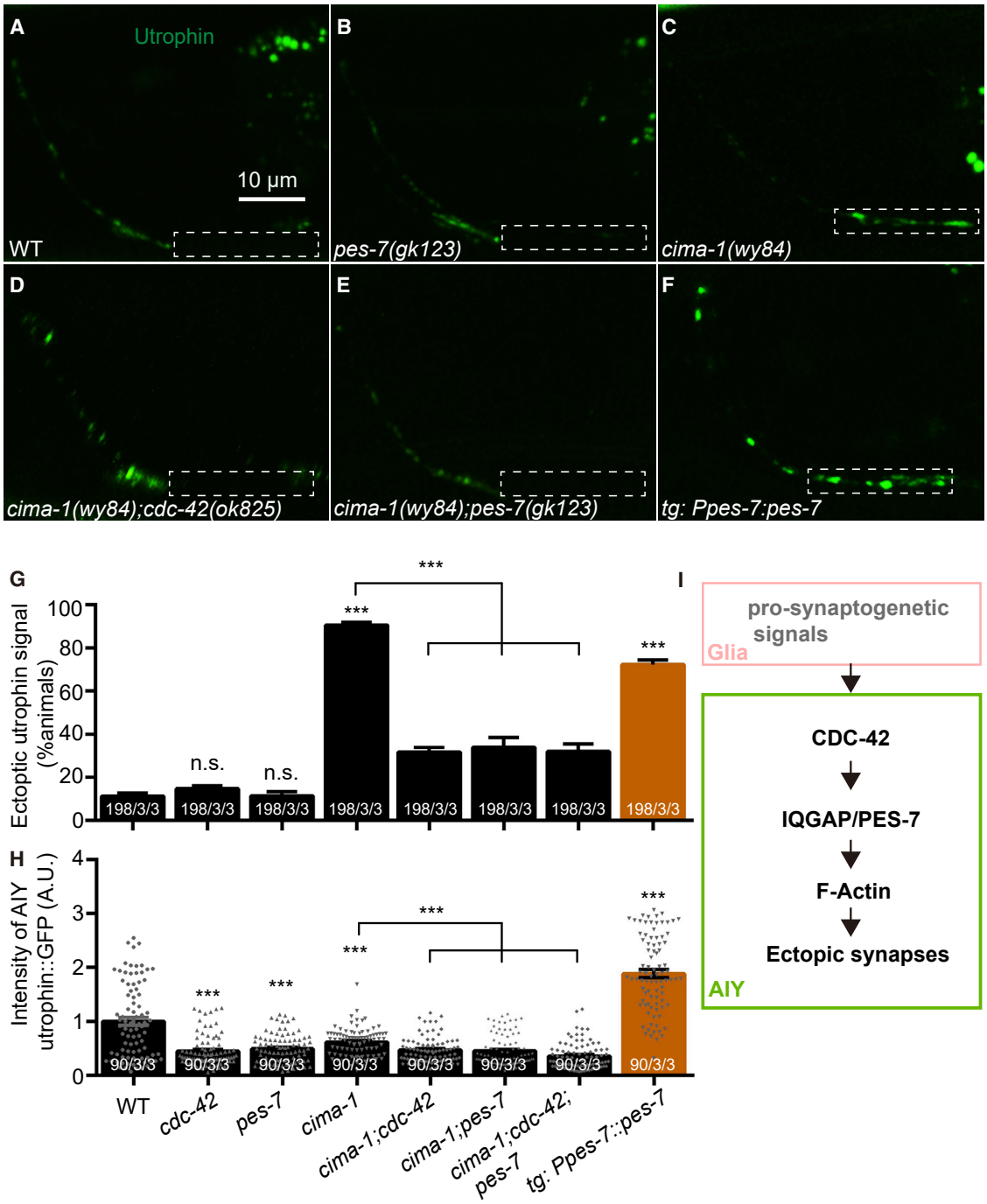

Figure 7. *pes-7* May Promote Synaptogenesis by Regulating F-Actin Assembly

(A–F) Confocal micrographs of AIY interneurons labeled with F-actin binding marker utrophin::GFP in WT (A), *pes-7(gk123)* (B), *cima-1(wy84)* (C), *cima-1(wy84);cdc-42(ok825)* (D), *cima-1(wy84);pes-7(gk123)* (E), and the P*pes-7::pes-7* transgene (F) animals. Dashed boxes mark zone 1 of the AIY interneurons. The scale bar (10 μm) in (A) applies to (B–F).

(G) Quantification of the percentage of animals with ectopic AIY GFP-tagged utrophin for the indicated genotypes.

(H) Quantification of utrophin::GFP intensity for the indicated genotypes.

(I) A model describing synaptic spatial specificity mediated by glia-neurons/CDC42-IQGAP. The total number of animals (N) and the replicates (n1) are indicated in each bar for each genotype, as they are for the transgenic lines created and the number of transgenic lines (n2) examined (all using the convention N/n1/n2). Statistical analysis is based on 1-way ANOVA followed by Dunnett's test. Error bars represent SEMs; n.s., not significant; ***$p < 0.001$.

CDC-42 and PES-7 are also functionally conserved. We speculate that presynaptic neuronal responses to synaptogenesis cues from VCSC glia apply to other animal systems.

STAR★METHODS

Detailed methods are provided in the online version of this paper and include the following:

- KEY RESOURCES TABLE
- LEAD CONTACT AND MATERIALS AVAILABILITY
- EXPERIMENTAL MODEL AND SUBJECT DETAILS
- METHOD DETAILS
  - Plasmids and transformation
  - RNA interference
  - Confocal microscopy and imaging analysis
- QUANTIFICATION AND STATISTICAL ANALYSIS
- DATA AND CODE AVAILABILITY

SUPPLEMENTAL INFORMATION

Supplemental Information can be found online at https://doi.org/10.1016/j.celrep.2020.01.102.

ACKNOWLEDGMENTS

We are grateful to Dr. D.A. Colón-Ramos; Dr. S. Cai; the Caenorhabditis Genetics Center (CGC), which is funded by the NIH Office of Research Infrastructure Programs (P40 OD010440) for strains and plasmids; Dr. W. Zou, Dr. M. Ding, and members of the Shao laboratory for their comments; and Dr. M. Zhou, Dr. Y. Shi, and Dr. M. Jiang from the Institute of Brain Science (IOBS) facility core at Fudan University. Illustrations in Figures 1A, S4A'', S4E'', S4I'', and S4M'' came from WormAtlas (https://www.wormatlas.org), with or without modification, with permission from Z.F. Altun and D.H. Hall. This work was supported by the Natural Science Foundation of China (31471026, 31872762), the Shanghai Municipal Science and Technology Major Project (no. 2018SHZDZX01), and ZJLab.

AUTHOR CONTRIBUTIONS

X.D. and Z.S. conceived and designed the project. X.D. and S.J. performed the experiments. X.D. and Z.S. analyzed the data and interpreted the results. X.D. and Z.S. wrote the manuscript.

DECLARATION OF INTERESTS

The authors declare no competing interests.

Received: June 15, 2019
Revised: November 11, 2019
Accepted: January 29, 2020
Published: February 25, 2020

REFERENCES

Ahmadian, M.R., Stege, P., Scheffzek, K., and Wittinghofer, A. (1997). Confirmation of the arginine-finger hypothesis for the GAP-stimulated GTP-hydrolysis reaction of Ras. Nat. Struct. Biol. *4*, 686–689.

Alan, J.K., Struckhoff, E.C., and Lundquist, E.A. (2013). Multiple cytoskeletal pathways and PI3K signaling mediate CDC-42-induced neuronal protrusion in C. elegans. Small GTPases *4*, 208–220.

Alan, J.K., Robinson, S.K., Magsig, K.L., Demarco, R.S., and Lundquist, E.A. (2018). The Atypical Rho GTPase CHW-1 Works with SAX-3/Robo To Mediate Axon Guidance in *Caenorhabditis elegans*. G3 (Bethesda) *8*, 1885–1895.

Altun, Z.F., Herndon, L.A., Wolkow, C.A., Crocker, C., Lints, R., and Hall, D.H. (2002–2019). WormAtlas. http://www.wormatlas.org.

Baldwin, K.T., and Eroglu, C. (2017). Molecular mechanisms of astrocyte-induced synaptogenesis. Curr. Opin. Neurobiol. *45*, 113–120.

Basherudin, N., and Curtis, M.D. (2006). Identification of positive GATEWAY expression clones when both the pENTRY and pDEST vectors contain the same marker for bacterial selection. CSH Protoc. (*2006*), pdb.prot4647.

Bijata, M., Labus, J., Guseva, D., Stawarski, M., Butzlaff, M., Dzwonek, J., Schneeberg, J., Böhm, K., Michaluk, P., Rusakov, D.A., et al. (2017). Synaptic Remodeling Depends on Signaling between Serotonin Receptors and the Extracellular Matrix. Cell Rep. *19*, 1767–1782.

Bosworth, A.P., and Allen, N.J. (2017). The diverse actions of astrocytes during synaptic development. Curr. Opin. Neurobiol. *47*, 38–43.

Brenner, S. (1974). The genetics of Caenorhabditis elegans. Genetics *77*, 71–94.

Brown, M.D., and Sacks, D.B. (2006). IQGAP1 in cellular signaling: bridging the GAP. Trends Cell Biol. *16*, 242–249.

Burkel, B.M., von Dassow, G., and Bement, W.M. (2007). Versatile fluorescent probes for actin filaments based on the actin-binding domain of utrophin. Cell Motil. Cytoskeleton *64*, 822–832.

Cao, D., Su, Z., Wang, W., Wu, H., Liu, X., Akram, S., Qin, B., Zhou, J., Zhuang, X., Adams, G., et al. (2015). Signaling Scaffold Protein IQGAP1 Interacts with Microtubule Plus-end Tracking Protein SKAP and Links Dynamic Microtubule Plus-end to Steer Cell Migration. J. Biol. Chem. *290*, 23766–23780.

Chai, G.S., Feng, Q., Wang, Z.H., Hu, Y., Sun, D.S., Li, X.G., Ke, D., Li, H.L., Liu, G.P., and Wang, J.Z. (2017). Downregulating ANP32A rescues synapse and memory loss via chromatin remodeling in Alzheimer model. Mol. Neurodegener. *12*, 34.

Chelur, D.S., and Chalfie, M. (2007). Targeted cell killing by reconstituted caspases. Proc. Natl. Acad. Sci. USA *104*, 2283–2288.

Chen, W., Lim, H.H., and Lim, L. (1993). The CDC42 homologue from Caenorhabditis elegans. Complementation of yeast mutation. J. Biol. Chem. *268*, 13280–13285.

Chia, P.H., Patel, M.R., and Shen, K. (2012). NAB-1 instructs synapse assembly by linking adhesion molecules and F-actin to active zone proteins. Nat. Neurosci. *15*, 234–242.

Chia, P.H., Chen, B., Li, P., Rosen, M.K., and Shen, K. (2014). Local F-actin network links synapse formation and axon branching. Cell *156*, 208–220.

Christopherson, K.S., Ullian, E.M., Stokes, C.C., Mullowney, C.E., Hell, J.W., Agah, A., Lawler, J., Mosher, D.F., Bornstein, P., and Barres, B.A. (2005). Thrombospondins are astrocyte-secreted proteins that promote CNS synaptogenesis. Cell *120*, 421–433.

Colón-Ramos, D.A. (2009). Synapse formation in developing neural circuits. Curr. Top. Dev. Biol. *87*, 53–79.

Colón-Ramos, D.A., Margeta, M.A., and Shen, K. (2007). Glia promote local synaptogenesis through UNC-6 (netrin) signaling in C. elegans. Science *318*, 103–106.

Dyer, J.O., Demarco, R.S., and Lundquist, E.A. (2010). Distinct roles of Rac GTPases and the UNC-73/Trio and PIX-1 Rac GTP exchange factors in neuroblast protrusion and migration in C. elegans. Small GTPases *1*, 44–61.

Gao, C., Frausto, S.F., Guedea, A.L., Tronson, N.C., Jovasevic, V., Leaderbrand, K., Corcoran, K.A., Guzmán, Y.F., Swanson, G.T., and Radulovic, J. (2011). IQGAP1 regulates NR2A signaling, spine density, and cognitive processes. J. Neurosci. *31*, 8533–8542.

Garrett, A.M., and Weiner, J.A. (2009). Control of CNS synapse development by gamma-protocadherin-mediated astrocyte-neuron contact. J. Neurosci. *29*, 11723–11731.

Gibson, D.G., Young, L., Chuang, R.Y., Venter, J.C., Hutchison, C.A., 3rd, and Smith, H.O. (2009). Enzymatic assembly of DNA molecules up to several hundred kilobases. Nat. Methods *6*, 343–345.

Göritz, C., Mauch, D.H., Nägler, K., and Pfrieger, F.W. (2002). Role of glia-derived cholesterol in synaptogenesis: new revelations in the synapse-glia affair. J. Physiol. Paris *96*, 257–263.

Gotta, M., Abraham, M.C., and Ahringer, J. (2001). CDC-42 controls early cell polarity and spindle orientation in C. elegans. Curr. Biol. *11*, 482–488.

Hedman, A.C., Smith, J.M., and Sacks, D.B. (2015). The biology of IQGAP proteins: beyond the cytoskeleton. EMBO Rep. *16*, 427–446.

Hedrick, N.G., Harward, S.C., Hall, C.E., Murakoshi, H., McNamara, J.O., and Yasuda, R. (2016). Rho GTPase complementation underlies BDNF-dependent homo- and heterosynaptic plasticity. Nature *538*, 104–108.

Hochstim, C., Deneen, B., Lukaszewicz, A., Zhou, Q., and Anderson, D.J. (2008). Identification of positionally distinct astrocyte subtypes whose identities are specified by a homeodomain code. Cell *133*, 510–522.

Huang, Z.J. (2006). Subcellular organization of GABAergic synapses: role of ankyrins and L1 cell adhesion molecules. Nat. Neurosci. *9*, 163–166.

Imai, F., Ladle, D.R., Leslie, J.R., Duan, X., Rizvi, T.A., Ciraolo, G.M., Zheng, Y., and Yoshida, Y. (2016). Synapse Formation in Monosynaptic Sensory-Motor Connections Is Regulated by Presynaptic Rho GTPase Cdc42. J. Neurosci. *36*, 5724–5735.

Jausoro, I., Mestres, I., Remedi, M., Sanchez, M., and Cáceres, A. (2012). IQGAP1: a microtubule-microfilament scaffolding protein with multiple roles in nerve cell development and synaptic plasticity. Histol. Histopathol. *27*, 1385–1394.

Jausoro, I., Mestres, I., Quassollo, G., Masseroni, L., Heredia, F., and Caceres, A. (2013). Regulation of spine density and morphology by IQGAP1 protein domains. PLoS One *8*, e56574.

Kamath, R.S., and Ahringer, J. (2003). Genome-wide RNAi screening in Caenorhabditis elegans. Methods *30*, 313–321.

Katz, M., Corson, F., Iwanir, S., Biron, D., and Shaham, S. (2018). Glia Modulate a Neuronal Circuit for Locomotion Suppression during Sleep in C. elegans. Cell Rep. *22*, 2575–2583.

Katz, M., Corson, F., Keil, W., Singhal, A., Bae, A., Lu, Y., Liang, Y., and Shaham, S. (2019). Glutamate spillover in C. elegans triggers repetitive behavior through presynaptic activation of MGL-2/mGluR5. Nat. Commun. *10*, 1882.

Kay, A.J., and Hunter, C.P. (2001). CDC-42 regulates PAR protein localization and function to control cellular and embryonic polarity in C. elegans. Curr. Biol. *11*, 474–481.

Kucukdereli, H., Allen, N.J., Lee, A.T., Feng, A., Ozlu, M.I., Conatser, L.M., Chakraborty, C., Workman, G., Weaver, M., Sage, E.H., et al. (2011). Control of excitatory CNS synaptogenesis by astrocyte-secreted proteins Hevin and SPARC. Proc. Natl. Acad. Sci. USA *108*, E440–E449.

Lee, I.J., Coffman, V.C., and Wu, J.Q. (2012). Contractile-ring assembly in fission yeast cytokinesis: recent advances and new perspectives. Cytoskeleton (Hoboken) *69*, 751–763.

Lin, Y.C., and Koleske, A.J. (2010). Mechanisms of synapse and dendrite maintenance and their disruption in psychiatric and neurodegenerative disorders. Annu. Rev. Neurosci. *33*, 349–378.

Locke, C.J., Kautu, B.B., Berry, K.P., Lee, S.K., Caldwell, K.A., and Caldwell, G.A. (2009). Pharmacogenetic analysis reveals a post-developmental role for Rac GTPases in Caenorhabditis elegans GABAergic neurotransmission. Genetics *183*, 1357–1372.

Lohmer, L.L., Clay, M.R., Naegeli, K.M., Chi, Q., Ziel, J.W., Hagedorn, E.J., Park, J.E., Jayadev, R., and Sherwood, D.R. (2016). A Sensitized Screen for Genes Promoting Invadopodia Function In Vivo: CDC-42 and Rab GDI-1 Direct Distinct Aspects of Invadopodia Formation. PLoS Genet. *12*, e1005786.

Martin-Vilchez, S., Whitmore, L., Asmussen, H., Zareno, J., Horwitz, R., and Newell-Litwa, K. (2017). RhoGTPase Regulators Orchestrate Distinct Stages of Synaptic Development. PLoS One *12*, e0170464.

Mateer, S.C., Morris, L.E., Cromer, D.A., Benseñor, L.B., and Bloom, G.S. (2004). Actin filament binding by a monomeric IQGAP1 fragment with a single calponin homology domain. Cell Motil. Cytoskeleton *58*, 231–241.

Mello, C., and Fire, A. (1995). DNA transformation. Methods Cell Biol. *48*, 451–482.

Melom, J.E., and Littleton, J.T. (2011). Synapse development in health and disease. Curr. Opin. Genet. Dev. *21*, 256–261.

Molofsky, A.V., Kelley, K.W., Tsai, H.H., Redmond, S.A., Chang, S.M., Madireddy, L., Chan, J.R., Baranzini, S.E., Ullian, E.M., and Rowitch, D.H. (2014). Astrocyte-encoded positional cues maintain sensorimotor circuit integrity. Nature *509*, 189–194.

Murakoshi, H., Wang, H., and Yasuda, R. (2011). Local, persistent activation of Rho GTPases during plasticity of single dendritic spines. Nature *472*, 100–104.

Muraoka, S., Shima, F., Araki, M., Inoue, T., Yoshimoto, A., Ijiri, Y., Seki, N., Tamura, A., Kumasaka, T., Yamamoto, M., and Kataoka, T. (2012). Crystal structures of the state 1 conformations of the GTP-bound H-Ras protein and its oncogenic G12V and Q61L mutants. FEBS Lett. *586*, 1715–1718.

Muthukumar, A.K., Stork, T., and Freeman, M.R. (2014). Activity-dependent regulation of astrocyte GAT levels during synaptogenesis. Nat. Neurosci. *17*, 1340–1350.

Narumiya, S. (1996). The small GTPase Rho: cellular functions and signal transduction. J. Biochem. *120*, 215–228.

Neniskyte, U., and Gross, C.T. (2017). Errant gardeners: glial-cell-dependent synaptic pruning and neurodevelopmental disorders. Nat. Rev. Neurosci. *18*, 658–670.

Neukomm, L.J., Zeng, S., Frei, A.P., Huegli, P.A., and Hengartner, M.O. (2014). Small GTPase CDC-42 promotes apoptotic cell corpse clearance in response to PAT-2 and CED-1 in C. elegans. Cell Death Differ. *21*, 845–853.

Qiu, R.G., Abo, A., and Steven Martin, G. (2000). A human homolog of the C. elegans polarity determinant Par-6 links Rac and Cdc42 to PKCzeta signaling and cell transformation. Curr. Biol. *10*, 697–707.

Rodal, A.A., Motola-Barnes, R.N., and Littleton, J.T. (2008). Nervous wreck and Cdc42 cooperate to regulate endocytic actin assembly during synaptic growth. J. Neurosci. *28*, 8316–8325.

Schrick, C., Fischer, A., Srivastava, D.P., Tronson, N.C., Penzes, P., and Radulovic, J. (2007). N-cadherin regulates cytoskeletally associated IQGAP1/ERK signaling and memory formation. Neuron *55*, 786–798.

Shao, Z., Watanabe, S., Christensen, R., Jorgensen, E.M., and Colón-Ramos, D.A. (2013). Synapse location during growth depends on glia location. Cell *154*, 337–350.

Shen, K., and Bargmann, C.I. (2003). The immunoglobulin superfamily protein SYG-1 determines the location of specific synapses in C. elegans. Cell *112*, 619–630.

Shi, Y., Kirwan, P., Smith, J., Robinson, H.P., and Livesey, F.J. (2012). Human cerebral cortex development from pluripotent stem cells to functional excitatory synapses. Nat. Neurosci. *15*, 477–486, S1.

Skop, A.R., Liu, H., Yates, J., 3rd, Meyer, B.J., and Heald, R. (2004). Dissection of the mammalian midbody proteome reveals conserved cytokinesis mechanisms. Science *305*, 61–66.

Smith, J.M., Hedman, A.C., and Sacks, D.B. (2015). IQGAPs choreograph cellular signaling from the membrane to the nucleus. Trends Cell Biol. *25*, 171–184.

Stavoe, A.K., and Colón-Ramos, D.A. (2012). Netrin instructs synaptic vesicle clustering through Rac GTPase, MIG-10, and the actin cytoskeleton. J. Cell Biol. *197*, 75–88.

Stavoe, A.K., Nelson, J.C., Martínez-Velázquez, L.A., Klein, M., Samuel, A.D., and Colón-Ramos, D.A. (2012). Synaptic vesicle clustering requires a distinct MIG-10/Lamellipodin isoform and ABI-1 downstream from Netrin. Genes Dev. *26*, 2206–2221.

Stogsdill, J.A., Ramirez, J., Liu, D., Kim, Y.H., Baldwin, K.T., Enustun, E., Ejikeme, T., Ji, R.R., and Eroglu, C. (2017). Astrocytic neuroligins control astrocyte morphogenesis and synaptogenesis. Nature *551*, 192–197.

Swiech, L., Blazejczyk, M., Urbanska, M., Pietruszka, P., Dortland, B.R., Malik, A.R., Wulf, P.S., Hoogenraad, C.C., and Jaworski, J. (2011). CLIP-170 and

IQGAP1 cooperatively regulate dendrite morphology. J. Neurosci. *31*, 4555–4568.

Tashiro, A., Minden, A., and Yuste, R. (2000). Regulation of dendritic spine morphology by the rho family of small GTPases: antagonistic roles of Rac and Rho. Cereb. Cortex *10*, 927–938.

Tolias, K.F., Duman, J.G., and Um, K. (2011). Control of synapse development and plasticity by Rho GTPase regulatory proteins. Prog. Neurobiol. *94*, 133–148.

Tsai, H.H., Li, H., Fuentealba, L.C., Molofsky, A.V., Taveira-Marques, R., Zhuang, H., Tenney, A., Murnen, A.T., Fancy, S.P., Merkle, F., et al. (2012). Regional astrocyte allocation regulates CNS synaptogenesis and repair. Science *337*, 358–362.

Wang, S., Watanabe, T., Noritake, J., Fukata, M., Yoshimura, T., Itoh, N., Harada, T., Nakagawa, M., Matsuura, Y., Arimura, N., and Kaibuchi, K. (2007). IQGAP3, a novel effector of Rac1 and Cdc42, regulates neurite outgrowth. J. Cell Sci. *120*, 567–577.

Watanabe, T., Wang, S., and Kaibuchi, K. (2015). IQGAPs as Key Regulators of Actin-cytoskeleton Dynamics. Cell Struct. Funct. *40*, 69–77.

Weissbach, L., Settleman, J., Kalady, M.F., Snijders, A.J., Murthy, A.E., Yan, Y.X., and Bernards, A. (1994). Identification of a human rasGAP-related protein containing calmodulin-binding motifs. J. Biol. Chem. *269*, 20517–20521.

White, E.L. (2007). Reflections on the specificity of synaptic connections. Brain Res. Brain Res. Rev. *55*, 422–429.

White, J.G., Southgate, E., Thomson, J.N., and Brenner, S. (1986). The structure of the nervous system of the nematode Caenorhabditis elegans. Philos. Trans. R. Soc. Lond. B Biol. Sci. *314*, 1–340.

Williams, M.E., de Wit, J., and Ghosh, A. (2010). Molecular mechanisms of synaptic specificity in developing neural circuits. Neuron *68*, 9–18.

Yogev, S., and Shen, K. (2014). Cellular and molecular mechanisms of synaptic specificity. Annu. Rev. Cell Dev. Biol. *30*, 417–437.

STAR★METHODS

KEY RESOURCES TABLE

REAGENT or RESOURCE	SOURCE	IDENTIFIER
Bacterial and Virus Strains		
Escherichia coli, OP50	*Caenorhabditis* Genetics Center	WormBase ID: OP50
Escherichia coli, DH5α	NCM Biotech	Cat#MD101-1
Escherichia coli, HT115	*Caenorhabditis* Genetics Center	WormBase ID: HT115(DE3)
Chemicals, Peptides, and Recombinant Proteins		
Trizol	Ambion	Cat#15596026
IPTG	Amresco	Cat#367-93-1
Muscimol	Tocris Bioscience	Cat#0289
Proteinase K	Emdchemicals	Cat#539480
Agar	Sigma	Cat#V900500
Peptone	Sigma	Cat#V900885
Tryptone	Sigma	Cat#LP0042
Yeast extract	Sigma	Cat#LP0021
Critical Commercial Assays		
Phanta® Max Super-Fidelity DNA Polymerase	Vazme	Cat#P505-d1
Zyppy Plasmid Miniprep Kit	ZYMO Reseach	Cat#D4020
Zymoclean Gel DNA Recovery Kit	ZYMO Reseach	Cat#D4008
GoScrip™ Reverse Transcription System	Promega	Cat#A5001
RQ1 RNase-FREE DNase Kit	Promega	Cat#M6101
Gateway BP Clonase II Enzyme Mix	Invitrogen	Cat#11789
Seamless Cloning Kit	Beyotime	Cat#D7010M
Experimental Models: Organisms/Strains		
See Table S2 for the detail strain information		N/A
Recombinant DNA		
See Table S3 for primer sequences and information		N/A
Software and Algorithms		
Imaris x64 7.6.5	N/A	https://imaris.oxinst.com/
Adobe Illustrator CC2019	N/A	https://www.adobe.com
Graphpad Prism5	N/A	https://www.graphpad.com
Adobe photoshop CC	N/A	https://www.adobe.com

LEAD CONTACT AND MATERIALS AVAILABILITY

Further information and requests for resources and reagents should be directed to and will be fulfilled by the Lead Contact Zhiyong Shao (shaozy@fudan.edu.cn). All *C. elegans* strains generated in this study are available on request from the Lead Contact.

EXPERIMENTAL MODEL AND SUBJECT DETAILS

C. elegans strains were cultured at 21°C on nematode growth media (NGM) agar plates seeded with *Escherichia coli* OP50 (Brenner, 1974). Bristol N2 is used as the wild-type background. The following mutant alleles were used in this study: *cima-1(wy84)* IV, *cdc-42(ok825)* II, *pes-7(gk123)* I. Strains used in this study are listed in Table S2. Animals were scored at adult day 1 stage unless specified.

METHOD DETAILS

Plasmids and transformation

Constructs were built with either the pSM vector (derivation of pPD49.26) (Shen and Bargmann, 2003), gateway system (Invitrogen), or L4440 for RNAi (Kamath and Ahringer, 2003). RNAi constructs were made by inserting target cDNA into the XmaI or *NotI* site of the

L4440. All *cdc-42* plasmids are made with the pSM (Shen and Bargmann, 2003). Endogenous and tissue specific *pes-7* rescue plasmids were generated with gateway system (Basherudin and Curtis, 2006). PES-7 truncation constructs were made by fragment recombination (Gibson et al., 2009). Detailed information is described in Table S3.

Transgenic strains were generated by microinjections as previously (Mello and Fire, 1995). We used the P*hlh-17::mCherry* (20ng/μl), P*unc-122::GFP* (20ng/μl) or P*unc-122::RFP* (20ng/μl) as coinjection markers. All transgenes and the corresponding concentrations of the plasmids are listed in Table S2.

RNA interference

Standard feeding RNAi screen was performed (Kamath and Ahringer, 2003). Briefly, bacteria HT115 carrying the empty vector L4440 or the same vector inserted with the target cDNA between the double T7 promoter that can generate the double strand mRNA to interfere the target gene expression were used as the nematode *C. elegans* food. Empty vector and *dpy-7*, a gene that suppresses *cima-1(wy84)* (Shao et al., 2013), were used as negative and positive controls. Synchronized L4 animals were fed with RNAi bacteria strains with the control vector or a vector expressing the target double strand mRNA until the F1 generation reaches adult day 1 for the synaptic phenotype scoring. FDU937 [*cima-1(wy84);wyIs45(Pttx-3::GFP::RAB-3)*] was used in the RNAi screen. Genes screened are listed in the Table S1.

Confocal microscopy and imaging analysis

Synchronized animals were anaesthetized with muscimol and mounted on 3% agarose pad for phenotyping or imaging. AIY ectopic synapses were those at the AIY zone 1 region indicated by dashed boxes in figures.

Images presented in this study were obtained using either Perkin Elmer UltraVIEW VoX or Andor Dragonfly Spinning Disc Confocal Microscope with 40x objectives, 488nm laser for GFP and 561nm laser for mCherry. For fluorescent intensity quantification, all images were taken with Andor Dragonfly Spinning Disc Confocal Microscope with 40x objective. The Z series of optical sections were acquired 0.5 μm step size. Adobe photoshop CC was used to rotate and crop the image.

QUANTIFICATION AND STATISTICAL ANALYSIS

We quantified the percentage of animals with ectopic synapses using a Nikon Ni-U fluorescent microscope. Animals were considered to have ectopic synapses when synaptic markers were detected in the AIY zone 1 region (Shao et al., 2013). At least three biological replicates were obtained for each quantification. The total number of animals, biological replicates and the number of extrachromosomal lines used are indicated in each bar of the graphs. Adult phenotypes were scored 24 hours after the larva L4 stage. For the larval phenotype, eggs collected within a two-hour window were cultured for 12, 21, 29, and 38 hours to reach the L1, L2, L3, and L4 stages. Imaris was used to quantify the total presynaptic fluorescence intensity. Data were obtained from at least two independent transgenic lines and three biological replicates. The ratio of presynaptic length was calculated as the sum of the lengths of zone 2 and the length of ectopic synapses in zone 1 divided by total synaptic length (b/(a+b), a and b are indicated in the Figures 1P–1R) (Shao et al., 2013). All quantitative data were collected blindly.

The graphical data are presented as mean ± SEM. Statistics for comparisons between two groups were performed with two-tailed Student's t tests. Comparisons among more than two groups were performed with one-way or two-way analyses of variance (ANOVA). Statistical analyses in this study were completed using GraphPad Prism software (version 5.0).

DATA AND CODE AVAILABILITY

This study did not generate any unique datasets or code.